Published in final edited form as:
Brain Res. 2008 November 6; 1239: 216–225. doi:10.1016/j.brainres.2008.08.075.

Differential sensitivity of human glioblastoma LN18 (PTEN-positive) and A172 (PTEN-negative) cells to Taxol for apoptosis

Ran Zhang[a], **Naren L. Banik**[a], and **Swapan K. Ray**[b,*]

[a]Department of Neurosciences, Medical University of South Carolina, Charleston, SC 29425, USA

[b]Department of Pathology, Microbiology and Immunology, University of South Carolina School of Medicine, Columbia, SC 29209, USA

Abstract

Glioblastoma is the most malignant brain tumors in humans and an average survival of glioblastoma patients hardly exceeds 12 months. Taxol is a plant-derived anti-cancer agent, which has been used in the treatments of many solid tumors. Deletion or mutation of phosphatase and tension homolog located on chromosome ten (PTEN) occurs in as high as 80% glioblastomas. We examined the sensitivity of human glioblastoma LN18 (PTEN-positive) and A172 (PTEN-negative) cells to Taxol for induction of apoptosis. Wright staining showed morphological features of apoptosis after treatment with different doses of Taxol for 24 h. Significant amount of apoptosis occurred in LN18 cells after treatment with 25 nM Taxol, while in A172 cells only after treatment with 50 nM Taxol. Western blotting with an antibody that could specifically detect activation or phosphorylation of Akt (p-Akt) did not show any p-Akt in LN18 cells but an increase in p-Akt in A172 cells. Activation of Akt in A172 cells could be reversed by pre-treatment of the cells with the phosphatidylinositol-3-kinase (PI3K) inhibitor LY294002, indicating involvement of PI3K activity in this process. Apoptosis occurred with an increase in Bax:Bcl-2 and mitochondrial release of cytochrome *c* into the cytosol leading to activation of mitochondria-dependent caspase cascade. Taxol did not cause upregulation of vascular endothelial growth factor (VEGF), a key mediator of angiogenesis, in LN18 cells but substantial upregulation of VEGF in A172 cells. After treatment with Taxol, increases in p-Akt and VEGF could maintain survival and angiogenesis, respectively, in PTEN-negative glioblastoma. As a single chemotherapy, Taxol might be more efficacious in PTEN-positive glioblastoma than in PTEN-negative glioblastoma. Thus, our study showed differential sensitivity of PTEN-positive and PTEN-negative glioblastoma cells to Taxol.

Keywords

Apoptosis; Cytochrome *c*; Glioblastoma; PTEN; Taxol; VEGF

*Correspondence to: Swapan K. Ray, Ph.D., Department of Pathology, Microbiology and, Immunology, University of South Carolina School of Medicine, 6439 Garners Ferry Road, Building 2, Room C11, Columbia, SC 29209, USA. Phone: +1-803-733-1593, Fax: +1-803-733-3192, E-mail: raysk8@gw.med.sc.edu.

1. Introduction

Taxol is one of the most powerful anti-cancer compounds among all chemotherapeutic drugs (Gligorov and Lotz, 2004). It is a plant-derived anti-cancer agent that has been efficacious in various solid tumors in preclinical studies (Rose, 1992; Geney et al. 2005; Das et al., 2008) as well as in clinical studies (Utsunomiya et al., 2006; Veltkamp et al., 2007). Taxol has been widely used for induction of apoptosis in many solid tumors (Gan et al., 1998; Gagandeep et al., 1999) including glioblastoma (Cahan et al., 1994; Das et al., 2008). It activates intrinsic pathway of apoptosis via mitochondrial release of cytochrome *c* into the cytosol leading to formation of apoptosome for activation of caspases (Jordan et al., 2004). Taxol is not so effective for treatment of recurrent glioblastoma even though it has shown great effectiveness in treatment of high-grade glioblastoma (Glantz et al., 1999; Rosenthanl et al., 2000). However, the anti-cancer efficacy of Taxol in glioblastoma can be significantly increased in combination with other therapeutic agents (Son et al., 2006; Karmakar et al., 2008) and also by increasing its transport across the blood-brain barrier (Fellner et al., 2002; Koziara et al., 2004). Recently, there is an excitement about the use of temozolomide for treatment of some glioblastomas that contain epigenetic silencing of the DNA repair gene O_6-methylguanine methyltransferase (Hegi et al., 2005). Even use of temozolomide alone may fail (Huang et al., 2008) or show only moderate efficacy (Yang et al., 2006) in recurrent and progressive glioblastomas. Temozolomide may also promote angiogenesis in glioblastomas (Fisher et al., 2007). So, research continues to advocate Taxol as an important choice for treatment of glioblastoma and identify the molecular makers that can modulate (increase or decrease) Taxol efficacy in glioblastoma. Apoptosis machinery does exist in glioblastomas (Ray et al., 2002). But recurrent glioblastomas may lack or harbor molecular markers of cell survival even when they are challenged with a powerful chemotherapeutic drug such as Taxol. Identification of such molecular markers that modulate cell survival in recurrent glioblastomas may help design rational therapeutics for their treatment.

Phosphatase and tensin homolog located on chromosome ten (PTEN), which encodes a cytoplasmic enzyme with both protein and lipid phosphatase activity, is frequently mutated or deleted at chromosome 10q23 in malignant glioblastomas (Ohgaki et al., 2007). Recent studies indicate that mutation and deletion of PTEN account for as high as 80% of human glioblastomas. Glioblastoma is the most prevalent and malignant brain tumor in humans and the average survival time of glioblastoma patients is less than 12 months even after treatment with currently available best therapeutic regimens (Jiang et al., 2007; Cloughesy et al., 2008). Angiogenesis is a crucial feature for the growth and progression of glioblastoma (Hanahan and Folkman, 1996; Kleihuses P et al, 1999). In comparison with other malignancies elsewhere in the body, glioblastoma is a notorious tumor due to its high capability of angiogenesis. Vascular endothelial growth factor (VEGF) plays a critical role in tumor angiogenesis and level of expression of VGEF correlates with the degree of malignancy of glioblastomas (Fischer et al., 2005; Reardon et al., 2008). Currently, it is a popular theory that attacking the tumor vascular bed instead of tumor cells themselves is an effective anti-tumor strategy due to low cytotoxicity and lack of drug resistance problem in this approach (Steiner et al., 2004). Transfection of PTEN to glioblatoma cells could decrease the secretion of VEGF (Gomez-Manzano et al., 2003).

Because of the modest anti-tumor activity of Taxol in some glioblastomas, we wanted to explore any potential role for the tumor suppressor PTEN in Taxol sensitivity in glioblastomas using human glioblastoma LN18 (PTEN-positive) and A172 (PTEN-negative) cells. Our findings suggest that dramatic difference in Taxol sensitivity for apoptosis in these two cell lines is due to their PTEN status. Presence of PTEN makes glioblastoma cells sensitive to Taxol, which also reduces the expression of VEGF in PTEN-positive cells but not in PTEN-negative cells. Notably, VEGF is an important angiogenic factor and primary focus of anti-

angiogenic interventions. Our study indicates that Taxol is a promising therapeutic agent for both induction of apoptosis and inhibition of angiogenic factor in PTEN-positive glioblastoma cells.

2. Results

2.1. Levels of PTEN expression in human glioblastoma LN18 and A172 cell lines

Overexpression of the tumor suppressor PTEN in malignant cells contributes to apoptosis and suppression of survival signaling. We examined levels of PTEN expression in LN18 and A172 cells after treatments with 25 nM and 50 nM Taxol (Fig. 1). The results demonstrated that treatments of LN18 cells with 25 nM and 50 nM Taxol induced PTEN expression (Fig. 1A) significantly ($p<0.01$) when compared with control cell (Fig. 1B). There was no detectable PTEN expression in A172 cells before and after the treatments. Treatment with Taxol did not induce activation or phosphorylation of Akt (p-Akt) in LN18 cells but caused significant increases in p-Akt expression in A172 cells (Fig. 1C and 1D). Treatment of A172 cells with LY294002, the phosphatidylinositol-3-kinase (PI3K) inhibitor, could significantly ($p<0.01$) prevent activation of Akt, indicating the involvement of PI3K activity in this process.

2.2. Taxol reduced cell viability and induced morphological and biochemical features of apoptosis

We determined amounts of residual cell viability and also apoptosis in LN18 and A172 cells after the treatments (Fig. 2).

Typan blue dye exclusion test was used to examine the residual cell viability in both LN18 and A172 cells after the treatments with 25 nM and 50 nM Taxol (Fig. 2A). Treatments with 25 nM and 50 nM Taxol significantly decreased ($p<0.01$) cell viability in LN18 cells but treatment with 50 nM Taxol significantly reduced ($p<0.05$) cell viability in A172 cells (Fig. 2A).

Wright staining was used to detect the morphologic characteristics of apoptosis such as cell shrinkage, membrane blebbing, chromatin condensation, and formation of membrane-bound apoptotic bodies in LN18 and A172 cells after the treatments (Fig. 2B). Both LN18 and A172 cell lines demonstrated significant apoptotic characteristics after Taxol treatments. The percentages of apoptosis were calculated in both cell lines following the treatments. Compared with control LN18 cells, 25 nM and 50 nM Taxol caused ($p<0.01$) 40% and 45% apoptosis, respectively (Fig. 3C). Compared with control A172 cells, only 50 nM Taxol caused significant ($p<0.05$) amount (24%) of apoptosis.

ApopTag assay was used to detect DNA fragmentation in apoptotic cells following Taxol treatments (Fig. 2D). ApopTag assay showed little or no brown color in control cells, indicating almost absence of apoptosis. Compared with control LN18 cells, 25 nM and 50 nM Taxol significantly ($p<0.01$) increased percentages (37% and 41%, respectively) of apoptotic cells (Fig. 2E). Compared with control A172 cells, only 50 nM caused significant ($p<0.05$) amount (25%) of apoptotic death (Fig. 2E).

We also found that a low dose (50 μM) and a high dose (100 μM) of temozolomide were effective in inducing cell death significantly in LN18 cells but non-significantly in A1272 cells (data not shown).

2.3. An increase in Bax:Bcl-2 ratio triggered apoptosis

Western blotting was used to examine the levels of expression of Bax and Bcl-2 proteins and determine the Bax:Bcl-2 ratio in LN18 and A172 cells after the treatments (Fig. 3). Both 25 nM and 50 nM Taxol increased expression of Bax and but decreased expression of Bcl-2 to

some extents in LN18 and A172 cells (Fig. 3A). Compared with control LN18 cells, 25 nM and 50 nM Taxol caused significant ($p<0.01$) increases in Bax:Bcl-2 ratio (Fig. 3B). Compared with control A172 cells, 25 nM and 50 nM Taxol also caused significant ($p<0.01$) increases in Bax:Bcl-2 ratio (Fig. 3B). A significant in increase in the Bax:Bcl-2 ratio after Taxol treatment indicated that cells were commited to trigger apoptotic process via mitochondrial pathway.

2.4. Mitochondrial release of cytochrome *c* into the cytosol leading to activation of caspase-9

We analyzed the mitochondrial and cytosolic fractions for assessment of mitochondrial release of cytochrome *c* into the cytosol by Western blotting (Fig. 4). Mitochondrial release of cytochrome c into the cytosol occurred in both LN18 and A172 cells after treatments with 25 nM and 50 nM Taxol (Fig. 4A). Compared with control cells, treatments with Taxol caused significant decreases in mitochondrial levels of cytochrome *c* (Fig. 4B) and concomitantly significant increases in cytosolic levels of cytochrome c (Fig. 4C), indicating mitochondrial release of cytochrome *c* into the cytosol in both LN18 and A172 cells. The mitochondrial release of cytochrome *c* into the cytosol could cause activation of caspase-9 (Fig. 5). Western blotting (Fig. 5A) showed significant ($p<0.01$) increases in active 37kD caspase-9 in LN18 and A172 cells after Taxol treatments (Fig. 5B). Further, colorimetric assay confirmed significant ($p<0.01$) increases in caspase-9 activity in both cell lines after Taxol treatments (Fig. 5C).

2.5. Activation of caspase-3 and increase in calpain and caspase-3 activities

The activation of caspase-9 could in turn activate the final executioner caspase-3 (Fig. 6). Western blotting (Fig. 6A) showed significant increases in active 20 kD caspase-3 fragment in LN18 and A172 cells after Taxol treatments (Fig. 6B). Subsequently, colorimetric assay also showed significant ($p<0.01$) increases in caspase-3 activity in both cell lines after Taxol treatments (Fig. 6C). Increased calpain and caspase-3 could work co-operatively to cause proteolysis of cellular key cytoskeletal protein in course of apoptosis (Fig. 7). Western blotting (Fig. 7A) detected the significant increases in calpain and caspase-3 activities in proteolysis of 270 kD α-spectrin to calpain-specific 145 kD spectrin breakdown product (SBDP) (Fig. 7B) and caspase-3-specific 120 kD SBDP (Fig. 7C), respectively, after Taxol treatments.

2.6. Changes in expression of VEGF and bFGF

VEGF is a key factor for changing tumor microenvironment and tumor angiogenesis. It has been reported previously that the expression of VEGF in glioblastoma is regulated in a PI3K-dependent manner (Maity et al., 2000). Because PTEN controls PI3K activity, level of PTEN may alter expression of VEGF and any other angiogenic factor. Expression of bFGF also contributes to tumor angiogenesis. We used Western blotting to examine any influence of PTEN status in changing levels of the potential angiogenic factors (VEGF and bFGF) in LN18 and A172 cells after Taxol treatments (Fig. 8). Western blotting (Fig. 8A) showed that 50 nM Taxol caused significant decrease in expression of VEGF (Fig. 8B) and no change in expression of bFGF (Fig. 8C) in PTEN-positive LN18 cells. On the other hand, Taxol treatments increased the levels of VEGF significantly (Fig. 8B) and bFGF non-significantly (Fig. 8C) in the PTEN-negative A172 cells.

3. Discussion

Glioblastoma, which is categorized amongst the most angiogenic tumors, is a highly vascularized and invasive malignant tumor with poor outcome even after treatment with the best therapeutic regimen (Kaur B et al., 2004). The dominant pro-angiogenic factor is VEGF that is widely used as a primary biomarker for determining efficacy of the anti-angiogenic interventions (Bello et al., 2004; Kargiotis et al., 2006). Since upto 80% glioblastomas have a deficiency of the tumor suppressor PTEN, the therapeutic outcome of an anti-glioblastoma

agent can be predicted based on levels of expression of PTEN and VEGF (Fan et al., 2002; Pore et al., 2003).

Taxol is a highly potent anti-tumor agent that is widely used to induce apoptosis in many solid tumors. We employed two different glioblastoma cell lines, the PTEN-positive LN18 and the PTEN-negative A172, to assess Taxol sensitivity for induction of apoptosis. Our data demonstrated that Taxol can cause overexpression of PTEN in LN18 cells but can not induce expression of PTEN in A172 cells (Fig. 1). In A172 cells, Taxol could incur the expression of p-Akt or Akt activation that could be reversed by pre-treatment of cells with the PI3K inhibitor LY294002 (Fig. 1), indicating the involvement of PI3K activity for Akt activation in absence of PTEN expression. This observation was similar to the earlier reports showing that the expression of PTEN controlled the PI3K/Akt pathway in glioblastoma (Parsons, 2004;Rong et al., 2005;Zhang et al., 2007).

Taxol induced different amounts of apoptosis in LN18 and A172 cells due to their different PTEN status. Apoptotic cells were detected on the basis of morphological (Wright staining) and biochemical (ApopTag assay) features (Fig. 2). Both low and high (25 nM and 50 nM, respectively) of Taxol caused significant apoptotic death in LN18 (PTEN-positive) cells while only high concentration Taxol induced apoptosis in A172 (PTEN-negative) cells. These results indicated that Taxol sensitivity was greater in the PTEN-positive cell line than in the PTEN-negative cell line.

We examined the changes in molecular events leading to differential amounts of apoptosis in LN18 and A172 cells after Taxol treatments. Taxol changed the levels of proapoptotic Bax and anti-apoptotic Bcl-2 in both LN18 and A172 cell lines (Fig. 3). Both low and high doses of Taxol could increase expression of Bax effectively in LN18 cells but not so effectively in A172 cells. We noticed a decrease in expression of Bcl-2 in LN18 cells while almost no discernible change in expression of Bcl-2 in A172 cells following Taxol treatments. Therefore, the Bax:Bcl-2 ratio (an indicator of commitment to apoptosis) was much higher in LN18 cells than in A172 cells after Taxol treatments. Less increase in Bax:Bcl-2 ratio indicated the weak efficacy of Taxol in the PTEN-negative glioblastoma cells. Earlier studies linked the lasting expression of anti-apoptotic Bcl-2 with the resistance to chemotherapy in cancer cells (Adams and Cory, 1998;Merighi et al., 2007).

Our results showing mitochondrial release of cytochrome c into the cytosol provided the evidence for occurrence of apoptosis through mitochondrial pathway (Fig. 4). Taxol induced more mitochondrial release of cytochrome *c* into the cytosol in LN18 cells than it did in A172 cells. Cytosolic cytochrome *c* promoted the activation of caspase-9 after Taxol treatment (Fig. 5). We performed Western blotting and colorimetric assay to observe increases in active 37 kD caspase-9 fragment and caspase-9 activity, respectively, after Taxol treatments. The low dose of Taxol was sufficient to cause the highest increases in caspase-9 activation and activity in LN18 cells while Taxol dose-dependently increased the caspase-9 activation and activity in A172 cells (Fig. 5). We also examined the increases in active 20 kD caspase-3 fragment and caspase-3 activity following Taxol treatments (Fig. 6). The low and high doses of Taxol were most efficacious in LN18 and A172 cells, respectively, for increasing the caspase-3 activation and activity. Similarly, the low and high doses of Taxol were the most effective in LN18 and A172 cells, respectively, for proteolysis of 270 kD α-spectrin to generate the calpain-specific 145 kD SBDP and caspase-3-specific 120 kD SBDP (Fig. 7). These results demonstrated that both low and high doses of Taxol in LN18 and A172 cells caused the highest increases in proteolytic activities of calpain and caspase-3. Therefore, presence of PTEN in LN18 cells appeared to help increase the sensitivity to Taxol for activation of proteolytic activities for apoptosis.

Because VEGF and bFGF are the critical angiogenic factors for promoting growth in glioblastoma, we examined the changes in levels of VEGF and bFGF in LN18 and A172 cells after Taxol treatments (Fig. 8). Taxol treatments significantly decreased expression of VEGF in LN18 cells but increased in A172 cells. It has previously been shown that transfection of PTEN into the glioblastoma U87 cells using retroviral vector could suppress tumor angiogenesis due to decrease in VEGF at mRNA level in vitro as well as in vivo (Wen et al., 2002; Abe et al., 2003). When compared with the PTEN-positive cells, the PTEN-negative ells showed high secretion of VEGF protein (Zundel et al., 2000;Edwards et al., 2008). Integrin-linked kinase (ILK) is a therapeutic target in cancer treatment. Studies demonstrated that the PTEN-positive cells were sensitive to ILK inhibitors than the PTEN-negative cells and also suggested that ILK inhibitors decreased VEGF secretion due to induction of PTEN expression (Edwards et al., 2008). Our data indicated that Taxol could decrease expression of VEGF significantly and bFGF to some extent in PTEN-positive LN18 cells but increased their levels in PTEN-negative A172 cells.

In conclusion, our current study demonstrated differential anti-cancer effects of Taxol in human glioblastoma LN18 (PTEN-positive) and A172 (PTEN-negative) cells. Activation of the cell survival PI3K/Akt signaling pathway and lasting expression of the anti-apoptotic Bcl-2 in PTEN-negative glioblastoma cells could confer resistance to Taxol chemotherapy. This study implies that absence of PTEN in reccurent glioblastomas may help avoid apoptosis and promote angiogenesis leading to overall poor prognosis of these glioblastomas even after treatment with a powerful chemotherapeutic drug such as Taxol.

4. Materials and methods

4.1. Materials

Human glioblastoma cell lines LN18 and A172 were purchased from the American Type Culture Collection (ATCC, Rockville, MD, USA). We obtained polyclonal IgG antibodies against PTEN from Cell Signaling Technologies (Danvers, MA, USA), cytochrome c from BD Biosciences (San Jose, CA, USA), and Bax, Bcl-2, VEGF, and bFGF from Santa Cruz Biotechnology (Santa Cruz, CA, USA). Monoclonal IgG antibody against a-spectrin was received from Affiniti (Exeter, UK).

4.2. Cell culture

Human glioblastoma LN18 and A172 cell lines were separately grown in DMEM supplemented with 10% fetal bovine serum (FBS) and 1% penicillin and streptomycin. Cells were seeded in 75-cm^2 flasks and incubated at 37°C in a fully-humidified atmosphere with 5% CO_2. Once the cells were 80% confluent, they were starved in DMEM with 1% FBS for 24 h and maintained in this low serum condition in course of all treatments. Cells were treated with 25 nM and 50 nM Taxol for 24 hours. After the treatments, cells were processed for assessments of residual cell viability, morphological and biochemical features of apoptosis, apoptosis-related proteins by Western blotting, and caspase activities by colorimetric assays.

4.3. Cell viability assay

After the treatments of cells with Taxol, trypan blue dye exclusion test was performed to evaluate the residual cell viability (Ray et al., 1999; 2006). Viable cells maintained membrane integrity and did not take up trypan blue. Cells with compromised cell membranes took up trypan blue and therefore were counted as dead. At least 600 cells in each treatment were counted in four different fields and the number of viable cells was calculated as percentage of the total cell population.

4.4. Wright staining for morphological features of apoptosis

Cells from all treatments were harvested and washed in PBS, pH 7.4, and sedimented onto the microscopic slides using the Centra CL2 centrifuge (IEC, Needham Heights, MA, USA) at 1000 rpm for 5 min. Cells were fixed for Wright staining, as we reported previously (Das et al., 2006). Cellular morphology was examined under the light microscopy to examine assess amount of apoptosis. Cells were considered apoptotic with the characteristics such as reduction in cell volume, condensation of the chromatin, and/or the presence of cell membrane blebbing. About 600 cells were counted in each treatment and the percentage of apoptotic cells was calculated.

4.5. ApopTag peroxidase assay for detection of apoptotic DNA fragmentation

For detection of DNA fragmentation as a biochemical marker of apoptosis, glioblastoma cells on the microscopic slides were subjected to the TdT-mediated dUTP nick-end labeling (TUNEL) using the ApopTag peroxidase assay kit (Intergen, Purchase, NY, USA), as we reported (Ray et al., 2006). In TUNEL staining, we used 3,3′-diaminobenzidine (DAB) as a peroxidase substrate. Cells with DNA fragmentation produced a brown product from oxidative polymerization and cyclization of DAB in the course of the ApopTag peroxidase assay. ApopTag-positive cells were brown in a pale green background and were considered as apoptotic cells. Experiments were conducted in triplicate and percentage of ApopTag-positive cells was determined by counting the brown cells from randomly selected fields under the light microscope.

4.6. Protein extraction and Western blotting

After the treatments, cells were lyzed in a buffer composed of 50 mM Tris-HCl, pH 7.4, 0.1 mM phenylmethylsulfonyl fluoride (PMSF), and 5 mM EGTA for extraction of cellular proteins. Concentration of total proteins was determined colorimetrically using Coomassie-Plus protein assay reagent (Pierce, Rockford, IL, USA). The samples were mixed with an equal volume of 2x loading buffer [125 mM Tris-HCl, pH 6.8, 4% sodium dodecyl sulfate (SDS), 20% glycerol, 200 mM 1,4-dithio-DL-threitol (DTT), and 0.02% bromophenol blue], boiled for 5 min, and loaded (40 μg/lane) onto the 4–20% gradient gels for the SDS-ployacrylamide gel electrophoresis (SDS-PAGE). After SDS-PAGE, the gels were blotted to Immunobilon-P nylon membrane. The blots were blocked in 5% non-fat milk, 0.1% Tween, Tris-HCl, pH 7.8, for 2 h at room temperature. Then the blots were incubated with a specific primary IgG antibody for 2 h at room temperature or overnight at cold room followed by alkaline horseradish peroxidase-conjugated secondary IgG antibody for 1 h. Blots were developed using the enhanced chemiluminescence (ECL) or ECL-Plus reagents (Amersham Pharmacia, Buckinghamshire, UK). The ECL autoradiograms were scanned on a PowerLook Scanner (Umax Technologies, Fremont, CA, USA) using Photoshop software (Adobe Systems, Seattle, WA, USA) and optical density (OD) of each band was determined using Quantity One software (Bio-Rad, Hercules, CA, USA).

4.7. Analysis of mitochondrial release of cytochrome c into the cytosol

Cells from each treatment were harvested, washed once with ice-cold PBS, and gently lyzed for 1 min in 50 μl ice-cold lysis buffer (250 mM sucrose, 1 mM EDTA, 0.05% digitonin, 25 mM Tris-HCl, pH 6.8, 1 mM DTT, 1 μg/ml leupeptin, 1 μg/ml pepstatin, 1 μg/ml aprotinin, 1 mM benzamidine, and 0.1 mM PMSF) following the standard procedure (Pique et al., 2004). Lysates were centrifuged at 12,000×g in cold (4°C) for 3 min to obtain pellet (the fraction containing mitochondria) and supernatant (the cytosolic extract without mitochondria). Pellet and supernatant were analyzed by Western blotting using cytochrome c antibody.

4.8. Colorimetric assays for measurement of caspase-9 and caspase-3 activities

Measurements of caspase-9 and caspase-3 activities in cells were performed with the commercially available colorimetric assay kits (Sigma Chemical, St. Louis, MO, USA). Proteolytic activities of caspase-9 and caspase-3 were assayed based on the release of p-nitroanilide (p-NA) from LEHD-p-NA and DEVD-p-NA, respectively. The concentration of the p-NA released from the substrate was calculated from the absorbance at 405 nm.

4.9. Statistical analysis

Results were analyzed using StatView software (Abacus Concepts, Berkeley, CA, USA) and compared using one-way analysis of variance (ANOVA) with Fisher's post hoc test. Data were presented as mean ± standard deviation (SD) of separate experiments ($n \geq 3$). Significant difference from control value was indicated by * ($p<0.05$) or ** ($p<0.01$). Significant difference between single and double treatments was indicated by # ($p<0.05$).

Acknowledgments

This work was supported in part by the R01 grants (CA-91460 and NS-57811) from the National Institutes of Health (Bethesda, MD, USA) and also by a Spinal Cord Injury Research Fund grant (SCIRF-0803) from the state of South Carolina to S.K.R.

REFERENCES

Abe T, Terada K, Wakimoto H, Inoue R, Tyminski E, Bookstein R, Basilion JP, Chiocca EA. PTEN decreases in vivo vascularization of experimental gliomas in spite of proangiogenic stimuli. Cancer Res 2003;63:2300–2305. [PubMed: 12727853]

Adams JM, Cory S. The Bcl-2 protein family: Arbiters of cell survivals. Science 1998;281:1322–1326. [PubMed: 9735050]

Bello L, Giussani C, Carrabba G, Pluderi M, Costa F, Bikfalvi A. Angiogenesis and invasion in gliomas. Cancer Treat. Res 2004;117:263–284. [PubMed: 15015565]

Cahan MA, Walter KA, Colvin OM, Brem H. Cytotoxicity of taxol in vitro against human and rat malignant brain tumors. Cancer Chemother. Pharmacol 1994;33:441–444. [PubMed: 7905792]

Cloughesy TF, Yoshimoto K, Nghiemphu P, Brown K, Dang J, Zhu S, Hsueh T, Chen Y, Wang W, Youngkin D, Liau L, Martin N, Becker D, Bergsneider M, Lai A, Green R, Oglesby T, Koleto M, Trent J, Horvath S, Mischel PS, Mellinghoff IK, Sawyers CL. Antitumor activity of rapamycin in a Phase I trial for patients with recurrent PTEN-deficient glioblastoma. PLoS Med 2008;5:e8. [PubMed: 18215105]

Das A, Banik NL, Ray SK. Mechanism of apoptosis with the involvement of calpain and caspase cascades in human malignant neuroblastoma SH-SY5Y cells exposed to flavonoids. Int. J. Cancer 2006;119:2575–2585. [PubMed: 16988947]

Das A, Banik NL, Ray SK. Retinoids induced astrocytic differentiation with down regulation of telomerase activity and enhanced sensitivity to taxol for apoptosis in human glioblastoma T98G and U87MG cells. J. Neurooncol 2008;87:9–22. [PubMed: 17987264]

Edwards LA, Woo J, Huxham LA, Verreault M, Dragowska WH, Chiu G, Rajput A, Kyle AH, Kalra J, Yapp D, Yan H, Minchinton AI, Huntsman D, Daynard T, Waterhouse DN, Thiessen B, Dedhar S, Bally MB. Suppression of VEGF secretion and changes in glioblastoma multiforme microenvironment by inhibition of integrin-linked kinase (ILK). Mol. Cancer Ther 2008;7:59–70. [PubMed: 18202010]

Fan X, Aalto Y, Sanko SG, Knuutila S, Klatzmann D, Castresana JS. Genetic profile, PTEN mutation and therapeutic role of PTEN in glioblastomas. Int. J. Oncol 2002;21:1141–1150. [PubMed: 12370766]

Fellner S, Bauer B, Miller DS, Schaffrik M, Fankhänel M, Spruss T, Bernhardt G, Graeff C, Färber L, Gschaidmeier H, Buschauer A, Fricker G. Transport of paclitaxel (Taxol) across the blood-brain barrier in vitro and in vivo. J. Clin. Invest 2002;110:1309–1318. [PubMed: 12417570]

Fischer I, Gagner JP, Law M, Newcomb EW, Zagzag D. Angiogenesis in gliomas: biology and molecular pathophysiology. Brain Pathol 2005;15:297–310. [PubMed: 16389942]

Fisher T, Galanti G, Lavie G, Jacob-Hirsch J, Kventsel I, Zeligson S, Winkler R, Simon AJ, Amariglio N, Rechavi G, Toren A. Mechanisms operative in the antitumor activity of temozolomide in glioblastoma multiforme. Cancer J 2007;13:335–344. [PubMed: 17921733]

Gagandeep S, Novikoff PM, Ott M, Gupta S. Paclitaxel shows cytotoxic activity in human hepatocellular carcinoma cell lines. Cancer Lett 1999;136:109–118. [PubMed: 10211948]

Gan Y, Wientjes MG, Au JL. Relationship between paclitaxel activity and pathobiology of human solid tumors. Clin. Cancer Res 1998;4:2949–2955. [PubMed: 9865905]

Geney R, Chen J, Ojima I. Recent advances in the new generation taxane anticancer agents. Med. Chem 2005;1:125–139. [PubMed: 16787308]

Glantz MJ, Chamberlain MC, Chang SM, Prados MD, Cole BF. The role of paclitaxel in the treatment of primary and metastatic brain tumors. Semin Radiat Oncol 1999;9:27–33. [PubMed: 10210537]

Gligorov J, Lotz JP. Preclinical pharmacology of the taxanes: implications of the differences. Oncologist 2004;9:3–8. [PubMed: 15161985]

Gomez-Manzano C, Fueyo J, Jiang H, Glass TL, Lee HY, Hu M, Liu JL, Jasti SL, Liu TJ, Conrad CA, Yung WK. Mechanisms underlying PTEN regulation of vascular endothelial growth factor and angiogenesis. Ann. Neurol 2003;53:109–117. [PubMed: 12509854]

Hanahan D, Folkman J. Patterns and emerging mechanisms of the angiogenic switch during tumorigenesis. Cell 1996;86:353–364. [PubMed: 8756718]

Hegi ME, Diserens AC, Gorlia T, Hamou MF, de Tribolet N, Weller M, Kros JM, Hainfellner JA, Mason W, Mariani L, Bromberg JE, Hau P, Mirimanoff RO, Cairncross JG, Janzer RC, Stupp R. MGMT gene silencing and benefit from temozolomide in glioblastoma. N. Engl. J. Med 2005;352:997–1003. [PubMed: 15758010]

Huang F, Kavan P, Guiot MC, Markovic Y, Roberge D. When temozolomide alone fails: adding procarbazine in salvage therapy of glioma. Can. J. Neurol. Sci 2008;35:192–197. [PubMed: 18574933]

Jiang Z, Pore N, Cerniglia GJ, Mick R, Georgescu MM, Bernhard EJ, Hahn SM, Gupta AK, Maity A. Phosphate and tensin homologue deficiency in glioblastoma confers resistance to radiation and temozolomide that is reversed by the protease inhibitor nelfinavir. Cancer Res 2007;67:4467–44473. [PubMed: 17483362]

Jordan MA, Wilson L. Microtubules as a target for anticancer drugs. Nat. Rev. Cancer 2004;4:253–265. [PubMed: 15057285]

Kargiotis O, Rao JS, Kyritsis AP. Mechanisms of angigenesis in gliomas. J. Neurooncol 2006;78:281–293. [PubMed: 16554966]

Karmakar S, Banik NL, Ray SK. Combination of all-trans retinoic acid and paclitaxel-induced differentiation and apoptosis in human glioblastoma U87MG xenografts in nude mice. Cancer 2008;112:596–607. [PubMed: 18098270]

Kaur B, Tan C, Brat DJ, Post DE, Van Meir EG. Genetic and hypoxic regulation of angiogenesis in gliomas. J. Neurooncol 2004;70:229–243. [PubMed: 15674480]

Kleihues P, Ohgaki H. Primary and secondary glioblastomas: from concept to clinical diagnosis. Neuro-oncology 1999;1:44–51. [PubMed: 11550301]

Koziara JM, Lockman PR, Allen DD, Mumper RJ. Paclitaxel nanoparticles for the potential treatment of brain tumors. J. Control Release 2004;99:259–269. [PubMed: 15380635]

Maity A, Pore N, Lee J, Solomon D, O'Rourke DM. Epidermal growth factor receptor transcriptionally up-regulates vascular endothelial growth factor expression in human glioblastoma cells via a pathway involving phosphatidylinositol 3'-kinase and distinct from that induced by hypoxia. Cancer Res 2000;60:5879–5886. [PubMed: 11059786]

Merighi S, Benini A, Mirandola P, Gessi S, Varani K, Leung E, Maclennan S, Baraldi PG, Borea PA. Hypoxia inhibits paclitaxel-induced apoptosis through adenosine-mediated phosphorylation of bad in glioblastoma cells. Mol. Pharmacol 2007;72:162–172. [PubMed: 17400763]

Ohgaki H, Kleihues P. Genetic pathways to primary and secondary glioblastoma. Am. J. Pathol 2007;170:1445–1453. [PubMed: 17456751]

Parsons R. Human cancer, PTEN and the PI-3 kinase pathway. Semin. Cell Dev. Biol 2004;15:171–176. [PubMed: 15209376]

Piqué M, Barragán M, Dalmau M, Bellosillo B, Pons G, Gil J. Aspirin induces apoptosis through mitochondrial cytochrome c release. FEBS Lett 2000;480:193–196. [PubMed: 11034327]

Pore N, Lius A, Haas-Kogan DA, O'Rourke DM, Maity A. PTEN mutation and epidermal growth factor receptor activation regulate vascular endothelial growth factor (VEGF) mRNA expression in human glioblastoma cells by transactivating the proximal VEGF promoter. Cancer Res 2003;63:236–241. [PubMed: 12517803]

Ray SK, Karmakar S, Nowak MW, Banik NL. Inhibition of calpain and caspase-3 prevented apoptosis and preserved electrophysiological properties of voltage-gated and ligand-gated ion channels in rat primary cortical neurons exposed to glutamate. Neuroscience 2006;139:577–595. [PubMed: 16504408]

Ray SK, Patel SJ, Welsh CT, Wilford GG, Hogan EL, Banik NL. Molecular evidence of apoptotic death in malignant brain tumors including glioblastoma multiforme: upregulation of calpain and caspase-3. J. Neurosci. Res 2002;69:197–206. [PubMed: 12111801]

Ray SK, Wilford GG, Crosby CV, Hogan EL, Banik NL. Diverse stimuli induce calpain overexpression and apoptosis in C6 glioma cells. Brain Res 1999;829:18–27. [PubMed: 10350526]

Reardon DA, Desjardins A, Rich JN, Vredenburgh JJ. The emerging role of anti-angiogenic therapy for malignant glioma. Curr. Treat. Options Oncol 2008;9:1–22. [PubMed: 18256938]

Rong Y, Post DE, Pieper RO, Durden DL, Van Meir EG, Brat DJ. PTEN and hypoxia regulate tissue factor expression and plasma coagulation by glioblastoma. Cancer Res 2005;65:1406–1413. [PubMed: 15735028]

Rose WC. Taxol: a review of its preclinical in vivo antitumor activity. Anticancer Drugs 1992;3:311–321. [PubMed: 1358264]

Rosenthal MA, Gruber ML, Glass J, Nirenberg A, Finlay J, Hochster H, Muggia FM. Phase II study of combination taxol and estramustine phosphate in the treatment of recurrent glioblastoma multiforme. J Neurooncol 2000;47:59–63. [PubMed: 10930101]

Sano T, Lin H, Chen X, Langford LA, Koul D, Bondy ML, Hess KR, Myers JN, Hong YK, Yung WK, Steck PA. Differential expression of MMAC/PTEN in glioblastoma multiforme: relationship to localization and prognosis. Cancer Res 1999;59:1820–1824. [PubMed: 10213484]

Son MJ, Song HS, Kim MH, Kim JT, Kang CM, Jeon JW, Park SY, Kim YJ, Groves MD, Park K, Kim JH, Nam DH. Synergistic effect and condition of pegylated interferon alpha with paclitaxel on glioblastoma. Int. J. Oncol 2006;28:1385–1392. [PubMed: 16685440]

Steiner HH, Karcher S, Mueller MM, Nalbantis E, Kunze S, Herold-Mende C. Autocrine pathways of the vascular endothelial growth factor (VEGF) in glioblastoma multiforme: clinical relevance of radiation-induced increase of VEGF levels. J Neurooncol 2004;66:129–138. [PubMed: 15015778]

Utsunomiya H, Akahira J, Tanno S, Moriya T, Toyoshima M, Niikura H, Ito K, Morimura Y, Watanabe Y, Yaegashi N. Paclitaxel-platinum combination chemotherapy for advanced or recurrent ovarian clear cell adenocarcinoma: a multicenter trial. Int. J. Gynecol. Cancer 2006;16:52–56. [PubMed: 16445610]

Veltkamp SA, Rosing H, Huitema AD, Fetell MR, Nol A, Beijnen JH, Schellens JH. Novel paclitaxel formulations for oral application: a phase I pharmacokinetic study in patients with solid tumours. Cancer Chemother. Pharmacol 2007;60:635–642. [PubMed: 17205304]

Wen S, Stolarov J, Myers MP, Su JD, Wigler MH, Tonks NK, Durden DL. PTEN controls tumor-induced angiogenesis. Proc. Natl. Acad. Sci. USA 2001;98:4622–4627. [PubMed: 11274365]

Yang SH, Kim MK, Lee TK, Lee KS, Jeun SS, Park CK, Kang JK, Kim MC, Hong YK. Temozolomide chemotherapy in patients with recurrent malignant gliomas. J. Korean Med. Sci 2006;21:739–744. [PubMed: 16891823]

Zhang R, Banik NL, Ray SK. Combination of all-*trans* retinoic acid and interferon- gamma suppressed PI3K/Akt survival pathway in glioblastoma T98G cells whereas NF-κB survival signaling in glioblastoma U87MG cells for induction of apoptosis. Neurochem. Res 2007;32:2194–2202. [PubMed: 17616812]

Zundel W, Schindler C, Haas-Kogan D, Koong A, Kaper F, Chen E, Gottschalk AR, Ryan HE, Johnson RS, Jefferson AB, Stokoe D, Giaccia AJ. Loss of PTEN facilitates HIF-1-mediated gene expression. Genes Dev 2000;14:391–396. [PubMed: 10691731]

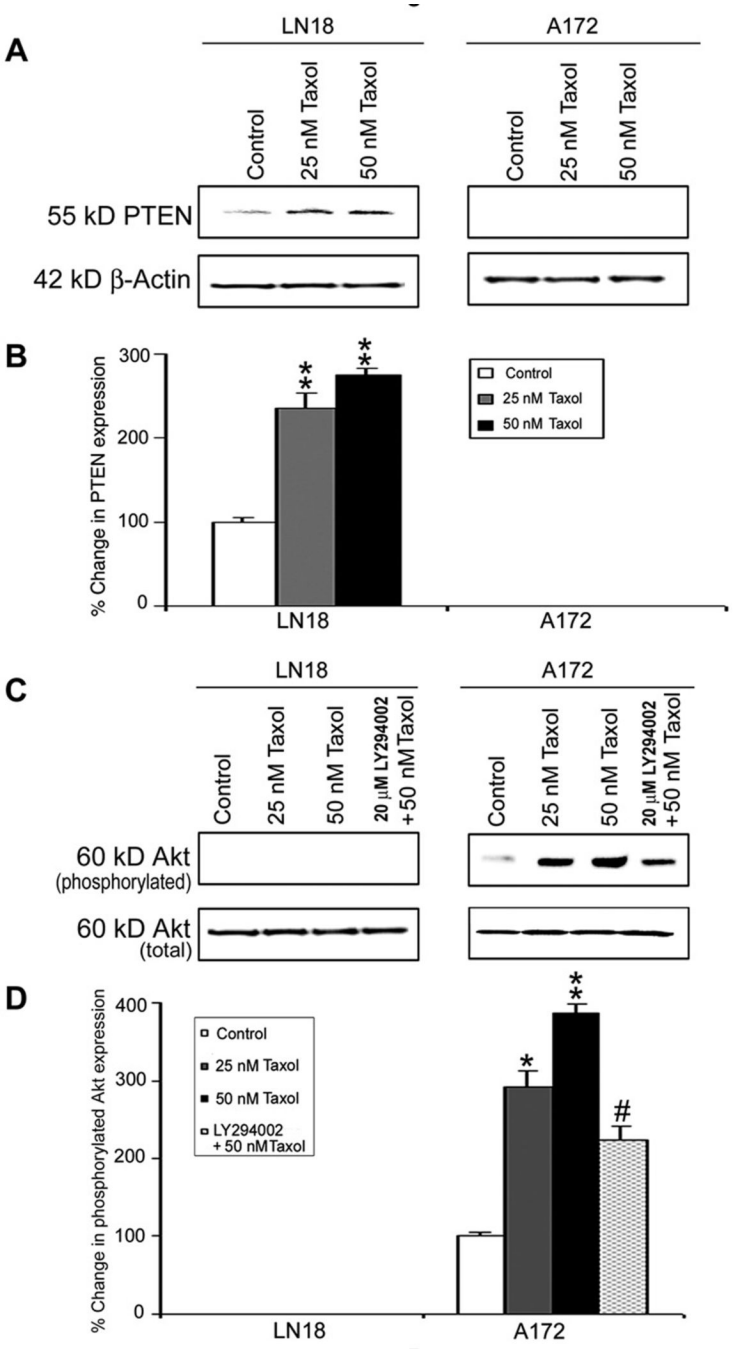

Fig. 1. Western blotting to assess levels of PTEN expression and activation of Akt in LN18 and A172 cells

(A) Representative Western blots showing levels of PTEN expression. (B) Densitometric determination of the levels of PTEN expression. (C) Representative Western blots showing activation or phosphorylation of Akt (p-Akt). (D) Densitometric determination of the levels of p-Akt. Treatments (24 h): Control, 25 nM Taxol, 50 nM Taxol, and 20 μM LY294002 (1 h pre-treatment) + 50 nM Taxol. Significant difference from control value was indicated by * ($p<0.05$) or ** ($p<0.01$). Significant difference between single and double treatments was indicated by # ($p<0.05$).

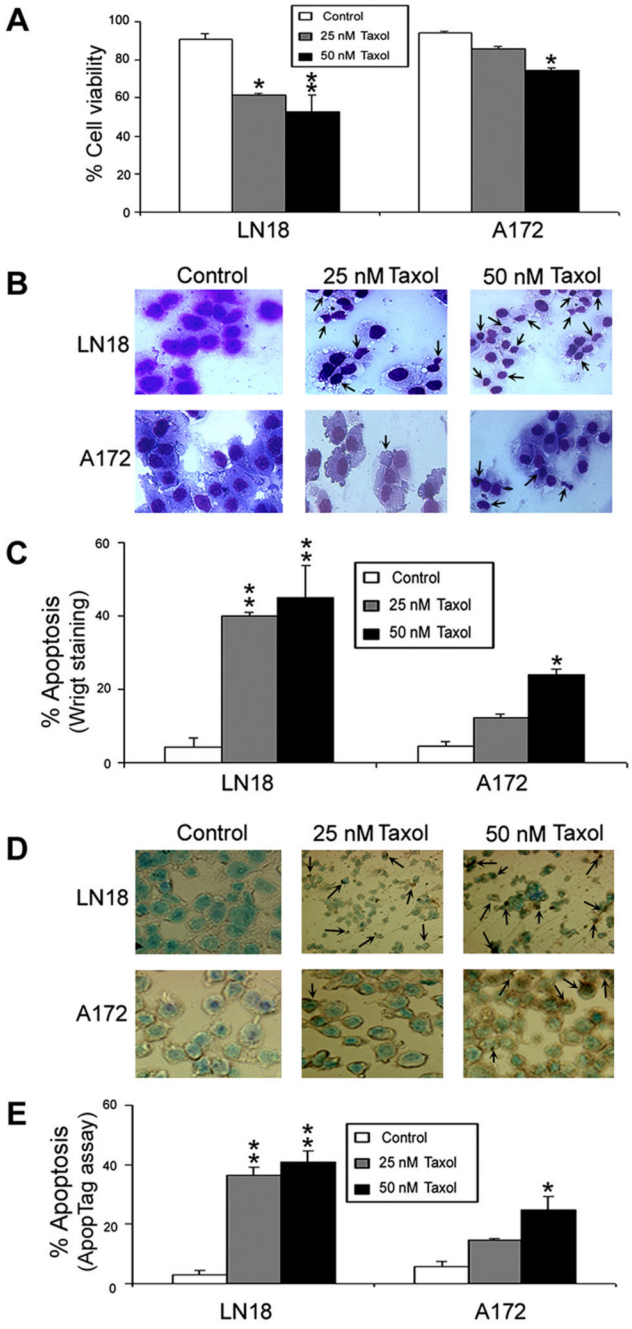

Fig. 2. Determination of residual cell viability and apoptosis in LN18 and A172 cells

Treatments (24 h): Control, 25 nM Taxol, and 50 nM Taxol. (A) Bar diagrams showing residual cell viability based on trypan blue dye exclusion test. (B) Wright staining to examine the morphological features of apoptotic cells (arrows). (C) Bar diagrams indicating percent apoptotic cells based on Wright staining. (D) ApopTag assay to examine the morphological features and DNA fragmentation in apoptotic cells (arrows). (E) Bar diagrams indicating percent apoptotic cells based on ApopTag assay. Significant difference from control value was indicated by *$p<0.05$ or **$p<0.01$.

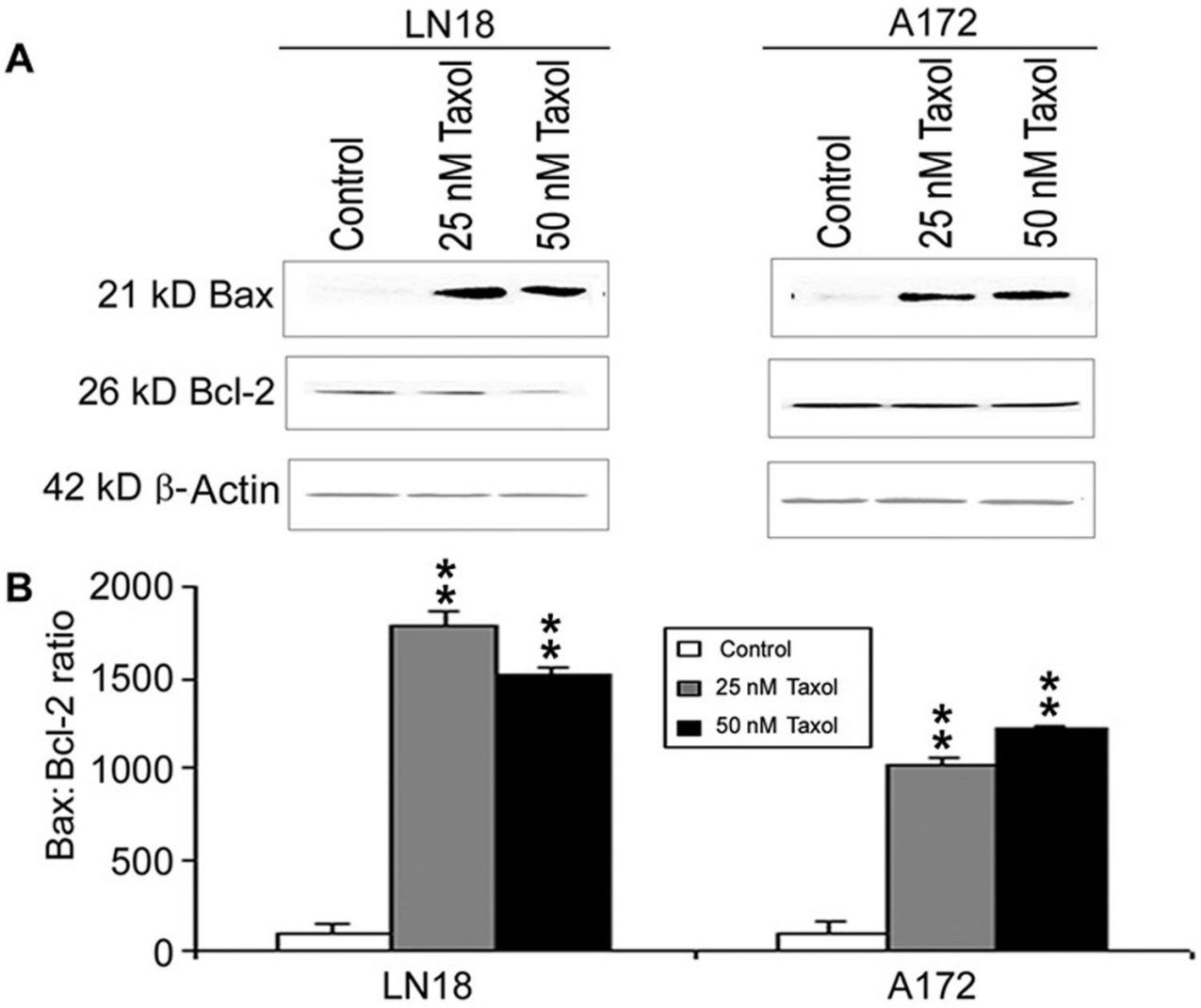

Fig. 3. Determination of Bax:Bcl-2 ratio in LN18 and A172 cells

Treatments (24 h): Control, 25 nM Taxol, and 50 nM Taxol. (A) Western blotting to show expression of pro-apoptotic Bax and anti-apoptotic Bcl-2 proteins. Expression of β-actin was monitored to ensure almost uniform protein loading in all lanes. (B) Bar diagram showing densitometric determination of the Bax:Bcl-2 ratio. Significant difference between control and a treatment was indicated by *$p<0.05$ or **$p<0.01$.

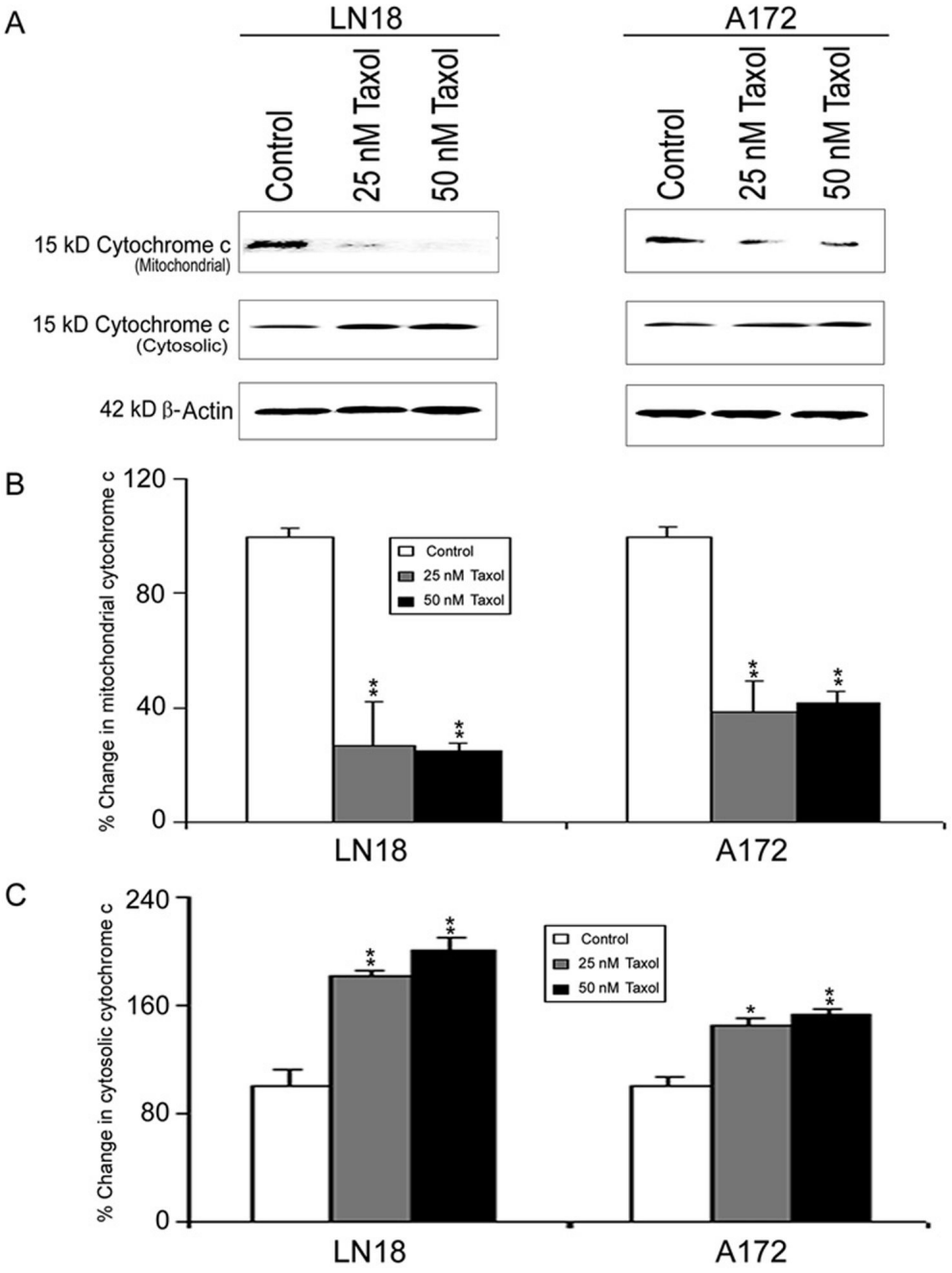

Fig. 4. Western blotting to examine mitochondrial release of cytochrome *c* into the cytosol in LN18 and A172 cells

Treatments (24 h): Control, 25 nM Taxol, and 50 nM Taxol. (A) Representative Western blots to show decrease in cytochrome *c* in mitochondria and increase in cytochrome *c* in the cytosol. Expression of β-actin was examined to ensure almost uniform protein loading in all lanes. (B) Bar diagrams to show densitometric determination of decreased levels of mitochondrial cytochrome *c*. (C) Bar diagram to show densitometric determination of increased levels of cytosolic cytochrome *c*. Significant difference between control and a treatment was indicated by *$p<0.05$ or **$p<0.01$.

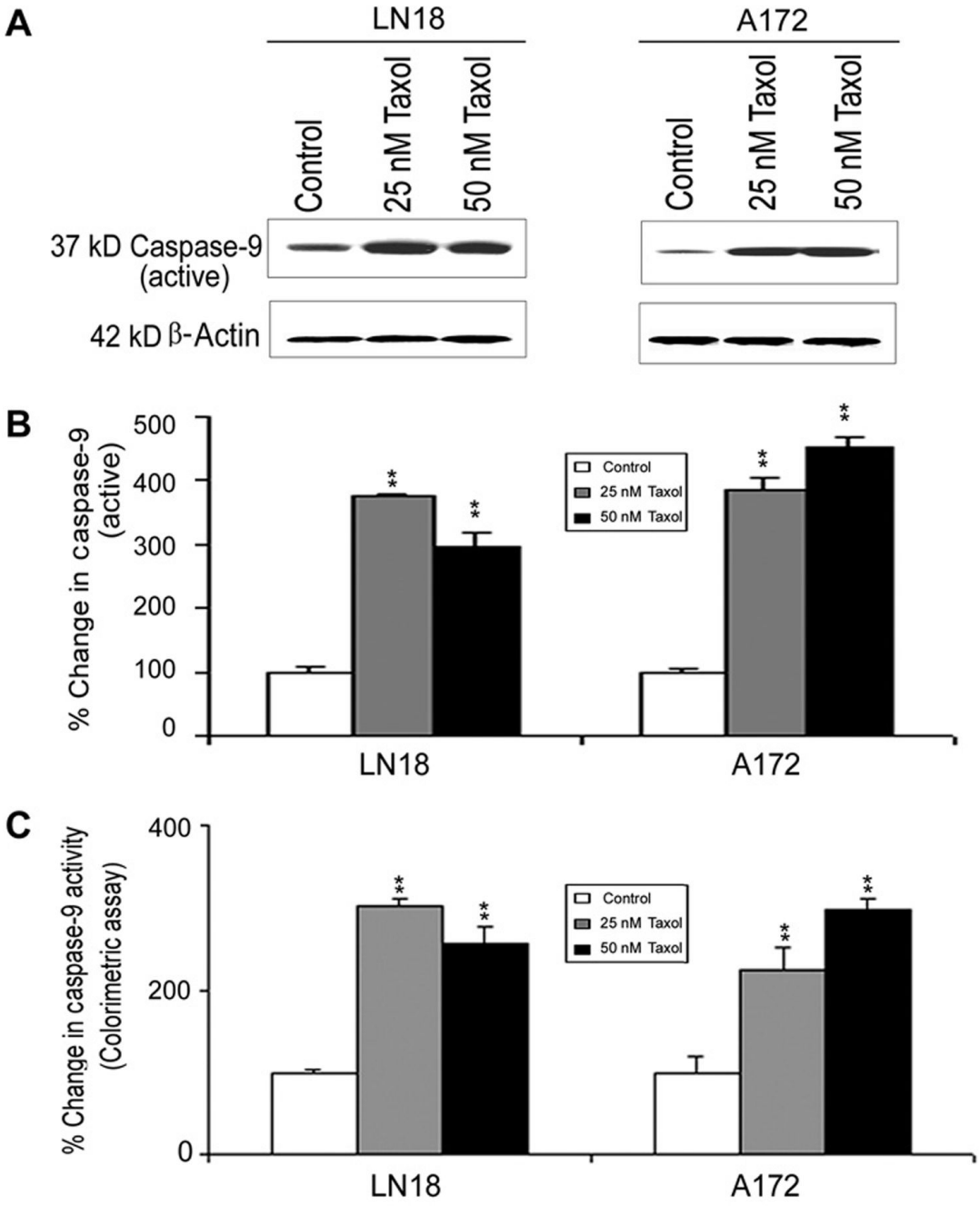

Fig. 5. Western blotting and colorimetric assay for determining caspase-9 activation and activity in LN18 and A172 cells

Treatments (24 h): Control, 25 nM Taxol, and 50 nM Taxol. (A) Representative Western blots to show increased levels of active caspase-9 expression. Expression of β-actin was examined to ensure almost uniform protein loading in all lanes. (B) Bar diagrams showing densitometric determination of levels of active caspase-9. (C) Colorimetric assay for determination of caspase-9 activity. Significant difference between control and a treatment was indicated by **$p<0.01$.

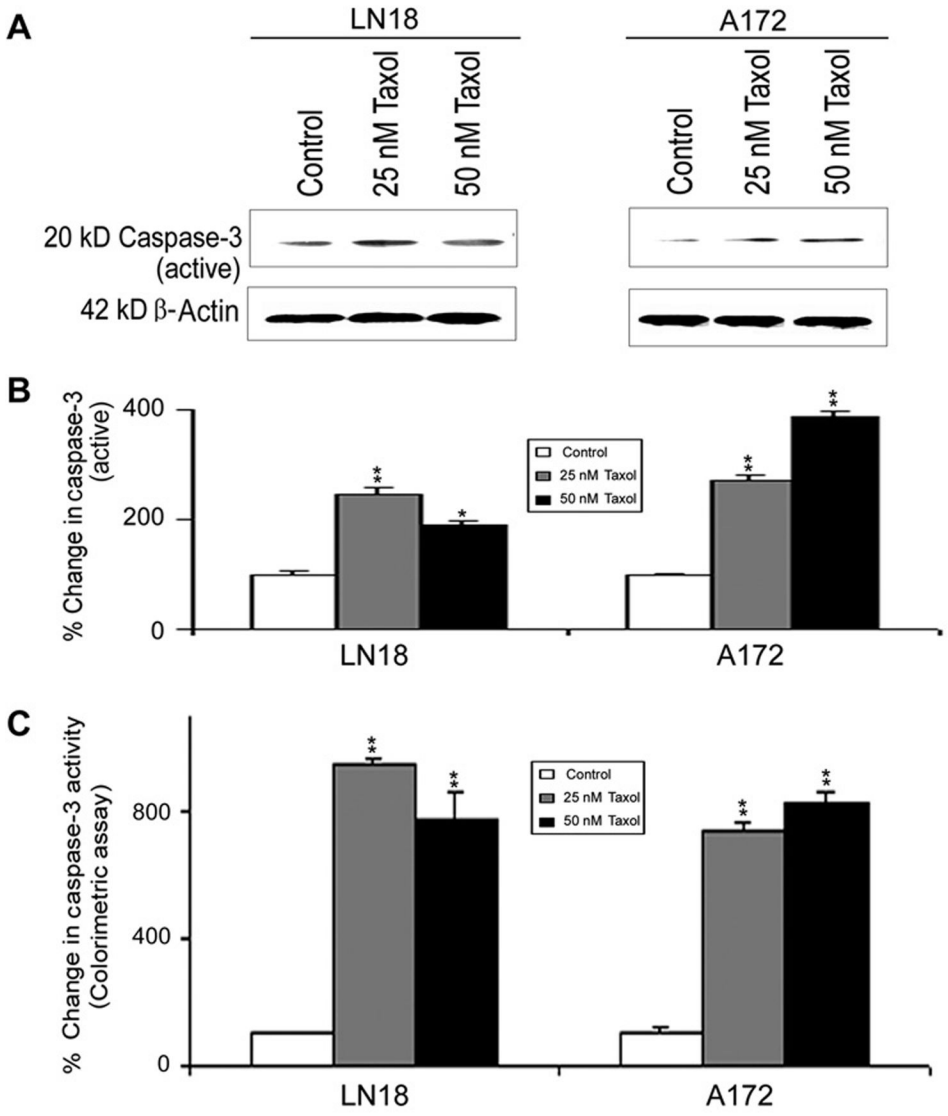

Fig. 6. Western blotting and colorimetric assay for determining caspase-3 activation and activity in LN18 and A172 cells

Treatments (24 h): Control, 25 nM Taxol, and 50 nM Taxol. (A) Representative Western blots to show increased levels of active caspase-3 expression. Expression of β-actin was examined to ensure almost uniform protein loading in all lanes. (B) Bar diagrams showing densitometric determination of levels of active caspase-3. (C) Colorimetric assay for determination of caspase-3 activity. Significant difference between control and a treatment was indicated by *$p<0.05$ or **$p<0.01$.

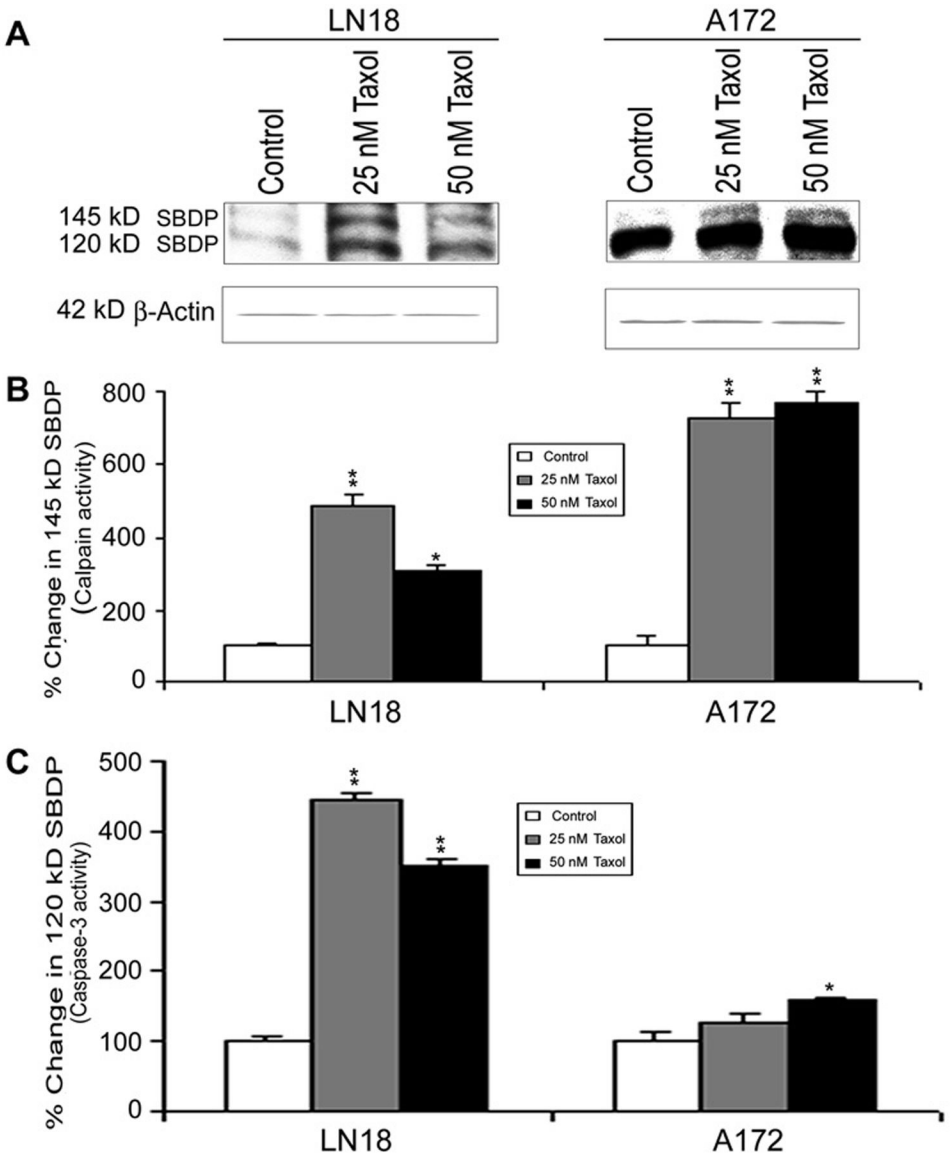

Fig. 7.

Western blotting to determine calpain and caspase-3 activities in a-spectin degradation in LN18 and A172 cells. Treatments (24 h): Control, 25 nM Taxol, and 50 nM Taxol. (A) Representative Western blots to show the appearance of calpain-specific 145 kD SBDP and caspase3-specific 120 kD SBDP indicating increased activities of calpain and caspase-3, respectively. Expression of β-actin was examined to ensure almost uniform protein loading in all lanes. (B) Bar diagrams to show densitometric determination of levels of 145 kD SBDP. (C) Bar diagrams to show densitometric determination of levels of 120 kD SBDP. Significant difference between control and a treatment was indicated by *$p<0.05$ or **$p<0.01$.

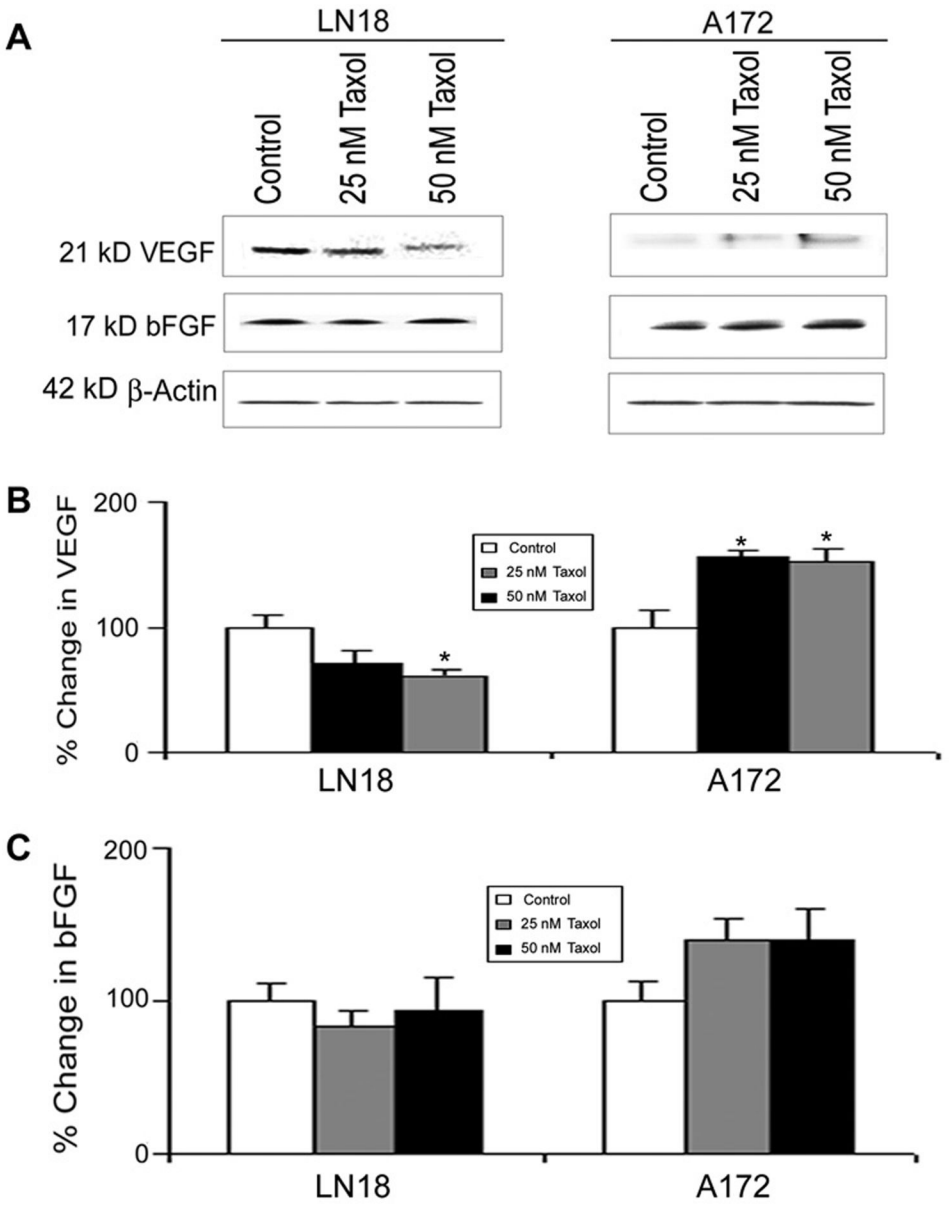

Fig. 8.

Western blotting to estimate levels of VEGF and bFGF in LN18 and A172 cells. (Treatments (24 h): Control, 25 nM Taxol, and 50 nM Taxol. (A) Representative Western blots to show the changes in levels of VEGF and bFGF. Expression of β-actin was examined to ensure almost uniform protein loading in all lanes. (B) Bar diagrams to show densitometric determination of levels of VEGF. (C) Bar diagrams to show densitometric determination of levels of bFGF. Significant difference from control value was indicated by *$p<0.05$.